Cyclic Hardening Behavior of Stainless Steel 316L - Experiments and Modeling

R. Halama [1,a], D. Ličková [1], J.J.R. Morales [2]

[1] *Department of Applied Mechanics, Faculty of Mechanical Engineering & National Supercomputing Centre IT4Innovations, VŠB - TU Ostrava, 17. listopadu 15, 70833 Ostrava, Czech Republic*
[2] *Universidad De Castilla - La Mancha, Calle Altagracia, 50, 13071 Ciudad Real, Cdad. Real, Spain*
[a] *radim.halama@vsb.cz*

Abstract: This paper shows main results of research emphasized on stress-strain behavior of the 316L stainless steel under proportional as well as non-proportional loading. The 316L steel shows significant additional hardening due to non-proportional loading. The results from all realized fatigue tests including the number of cycles to crack initiation and cyclic hardening/softening curves are presented. Two ways of fatigue parameters estimation are applied with comparable results. Important conclusions for the cyclic plasticity modeling considering investigated material are also discussed with emphasize on observed Non-Masing behavior and strain range dependent cyclic hardening.

Keywords: multiaxial fatigue; additional hardening; cyclic plasticity; 316L stainless steel.

1 Introduction

In the classical theory of plasticity the non-proportional loading is defined as a type of loading when principal stress directions rotate. The intensive research in the field of cyclic plasticity in last 30 years have shown that in case of non-proportional loading the cyclic hardening/softening behavior is more significant than in case of equivalent proportional loading [1]. Cyclic plasticity models based on phenomenological approach have to be very robust to describe cyclic hardening properties correctly under proportional as well as non-proportional loading [2]. The situation becomes more complicated in the case of stainless steels, because their transient behavior is strain range dependent [3]. Moreover, such cyclic plasticity model contains a large number of parameters which need to be estimated using a large number of experimental data from fatigue tests. This paper is focused on the stress-strain behavior investigation of the 316L stainless steel emphasizing the additional hardening behavior and the strain range dependent cyclic hardening.

2 Experimental study

All experiments were conducted on the 316L stainless steel. The electro-servo-hydraulic testing machine LabControl 100kN/1000Nm placed at the Faculty of Mechanical Engineering of the VŠB - Technical university of Ostrava was used for all cases.

The EPSILON extensometer - type 3550 with 25.4mm gauge length was used to measure/control the axial and shear strain simultaneously. For biaxial testing the specimen has tubular active part with outer and inner diameter of 12.5 mm and 10 mm respectively. The uniaxial fatigue tests were realized on solid round-type specimen with diameter of 5 mm. All low-cycle fatigue tests were realized on smooth specimens under strain control with zero mean strain during the cycle. The strain rate of about $6 \cdot 10^{-3}$ s^{-1} was considered in all tests during cycling. The number of cycles realized before crack initiation was determined in all tests based on the decrease of force (moment) amplitude of twenty percent in comparison to the saturated values. All experiments were performed at room temperature. The loading paths considered in this study are presented schematically in Fig.1. Eight different cases were realized. These paths were considered: uniaxial (case A), torsional (B), proportional (C), square (D), rhombic (E), two blocks (F), circular (G) and elliptical (H). The elliptical path shape corresponds to the 45° out of phase fatigue test.

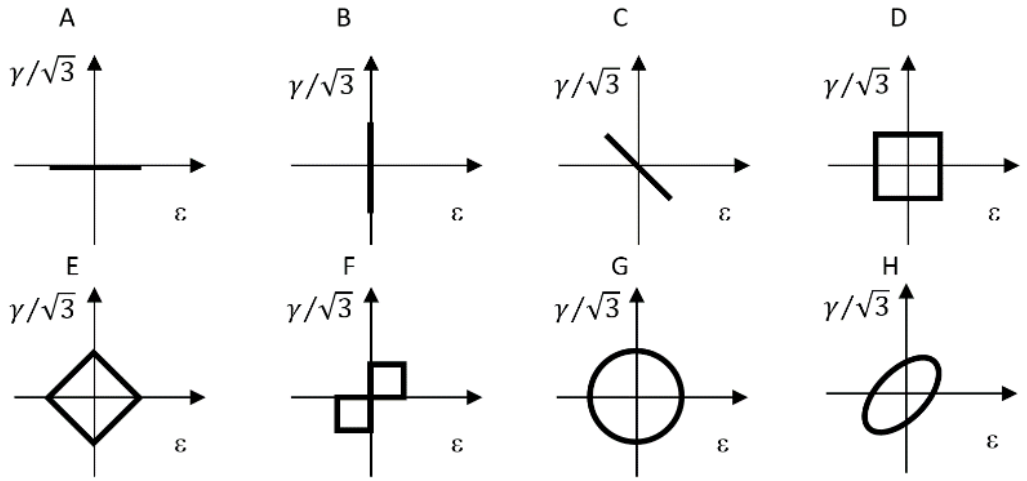

Fig. 1: Strain path shapes in particular cases

2.1 Uniaxial fatigue tests

In total nine low-cycle fatigue tests with constant amplitude of total strain were performed. The results of tests are summarized for all levels of loading in the Tab.1. Stable hysteresis loops evaluated in a half of fatigue life are displayed in the graph at the Fig.2. The Non-Masing behavior of the SS316L material is obvious from the Fig.2. It can be caused by a primary creep even under room temperature, which is well known phenomenon of stainless steels.

Tab. 1: Results of uniaxial fatigue tests.

Total strain amplitude ε_{at} [1]	Stress amplitude σ_a [MPa]	Number of cycles to failure N_f [1]
0.02433	627	24
0.01752	564	56
0.01349	501	133
0.00989	466	594
0.00699	424	897
0.00488	380	5700
0.00395	362	8630
0.00293	336	124450
0.00265	322	536512

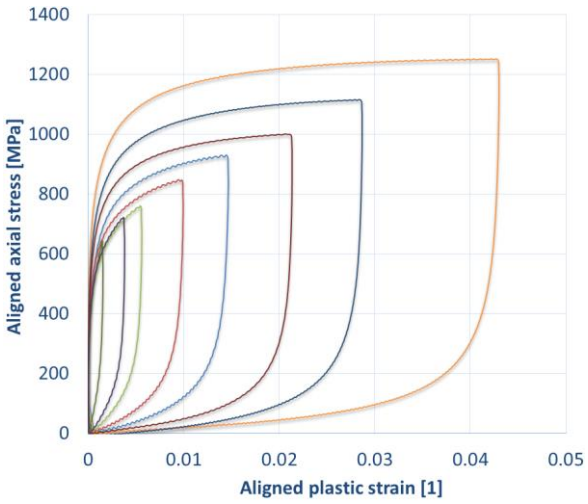

Fig. 2: Saturated hysteresis loops of SS316L alligned to the bottom peak

2.1.1 Uniaxial stress-strain behavior

The evolution of stress amplitude during cycling for selected levels of strain amplitude can be seen in the Fig.3. The investigated material reveals very rapid cyclic hardening in initial cycles followed by slow process of the cyclic softening.

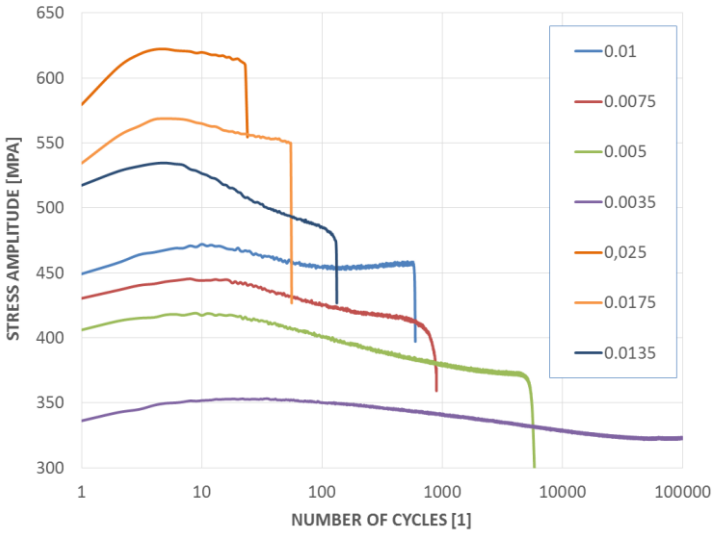

Fig. 3: Cyclic hardening/softening curves of SS316L for certain strain amplitudes

2.1.2 Fatigue parameters estimation methods

For evaluation of tests of low cycle fatigue in tension-compression, the Manson-Coffin-Basquin equation [4] is usually applied. It illustrates the relationship between the amplitude of total strain ε_{at} and number of cycles to crack initiation N_f

$$\varepsilon_{at} = \varepsilon_{ae} + \varepsilon_{ap} = \frac{\sigma_f'}{E}\left(2N_f\right)^b + \varepsilon_f'\left(2N_f\right)^c, \tag{1}$$

where ε_{ae} is the amplitude of elastic strain, ε_{ap} is the amplitude of plastic strain, ε_f' is the fatigue ductility coefficient, c is the fatigue ductility exponent, σ_f' is the fatigue strength coefficient and b is called as the fatigue strength exponent. The Young modulus was evaluated as a dynamic elastic modulus from all uniaxial stable hysteresis loops E=169785MPa. Amplitude of the total strain can be also expressed by the Ramberg-Osgood equation [5] as a function of stress amplitude in the case of tension-compression

$$\varepsilon_{at} = \varepsilon_{ae} + \varepsilon_{ap} = \frac{\sigma_a}{E} + \left(\frac{\sigma_a}{K'}\right)^{n'}, \tag{2}$$

where K' is the cyclic strength coefficient and n' is the cyclic strain hardening exponent.

Six fatigue constants have been usually determined by the conventional method based on approximation of the experimentally obtained data by a line (three independent linear regressions). Niesłony [6] has proposed a new method for identifying fatigue constants, the so-called 3D method. The main advantage of this method is that it ensures the compatibility of six fatigue constants. The method is based on the approximation by a straight line in xyz space, where $\mathrm{x} = log\left(\varepsilon_{ap}\right)$, $\mathrm{y} = log(\sigma_a)$, $\mathrm{z} = log(2N_f)$. The regression line is determined by the direction r $(\mathrm{r}_1, \mathrm{r}_2, \mathrm{r}_3)$ and a point P $(\mathrm{x_P}, \mathrm{y_P}, \mathrm{z_P})$, see Fig.4. Based on the direction vector coordinates and coordinates of point P the six fatigue coefficients are calculated as follows

$$n' = \frac{\mathrm{r}_2}{\mathrm{r}_1}, \tag{3}$$

$$K' = 10^{\mathrm{y_P} - \mathrm{x_P} n'}, \tag{4}$$

$$c = \frac{\mathrm{r}_1}{\mathrm{r}_3}, \tag{5}$$

$$\varepsilon_f' = 10^{\mathrm{x_P} - \mathrm{z_P} c}, \tag{6}$$

$$b = \frac{\mathrm{r}_2}{\mathrm{r}_3}, \tag{7}$$

$$\sigma_f' = 10^{\mathrm{y_P} - \mathrm{z_P} b}. \tag{8}$$

When solving the problem, 4 regressions are made. The first regression determines the equation of a plane in space and the other three are used to calculate regression lines in the planes $\mathbf{x} - \mathbf{y}$, $\mathbf{y} - \mathbf{z}$ and $\mathbf{z} - \mathbf{x}$, where $\mathbf{x} = \boldsymbol{log}(\boldsymbol{\varepsilon_{ap}})$, $\mathbf{y} = \boldsymbol{log}(\boldsymbol{\sigma_a})$, $\mathbf{z} = \boldsymbol{log}(\boldsymbol{2N_f})$. Subsequently, two regressions with the highest coefficient of determination are selected. It is obvious that at least one of the selected regressions is a line in plane, i.e. it is necessary to establish a plane which is given by the straight line and which is, at the same time, perpendicular to the plane in which it lies. In order to make methods more comfortable for use, there was developed algorithm in MATLAB.

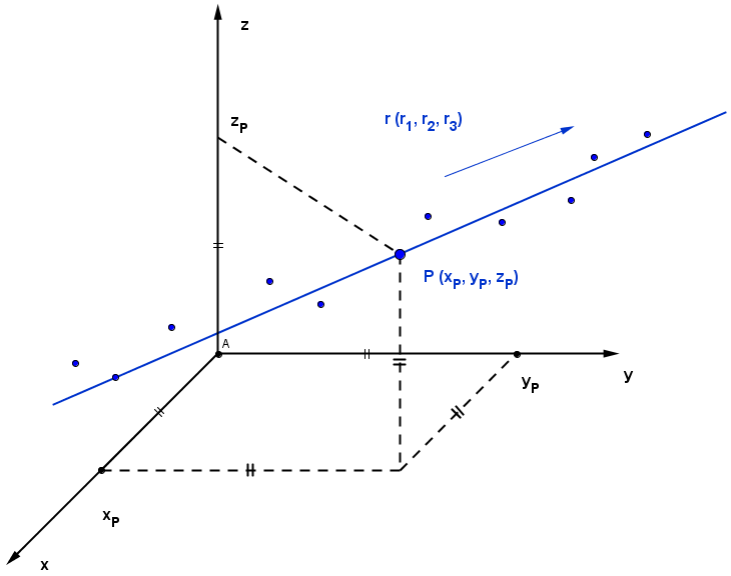

Fig. 4: Points in the 3D space with regression line determined by point P and directional vector r

2.1.3 Results of fatigue parameters estimation

Both methods (conventional and 3D method) were applied to obtain fatigue parameters of SS316L material. The resulting regression dependencies for the stainless steel 316L based on uniaxial data are shown as output from the MATLAB program in Fig.5. Values of fatigue constants obtained after application of the 3D and the conventional methods are presented in Tab. 2.

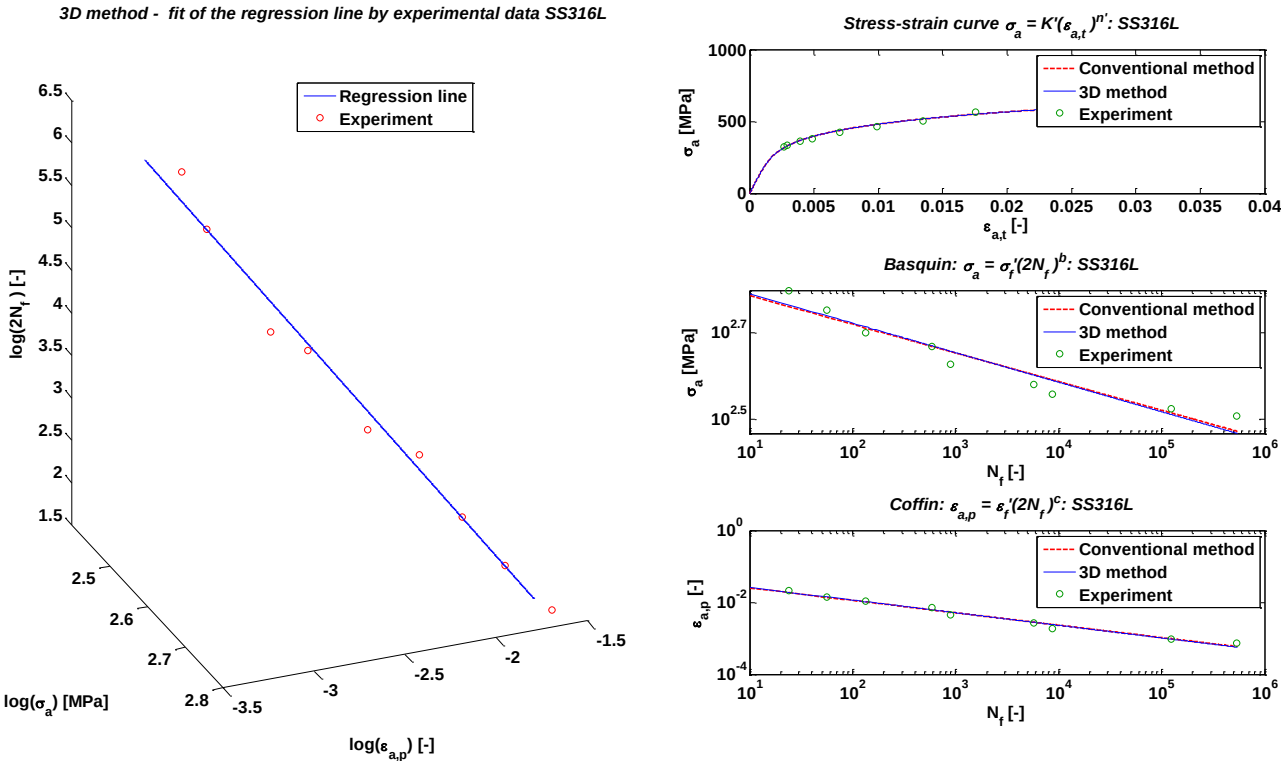

Fig.5: Graphical representation of 3D method application and its comparison with conventional method for the stainless steel 316L – tension-compression

Tab. 2: Results of 3D method and conventional method application.

Parameter	Conventional method	3D method
ε'_f	0.070	0.074
c	-0.343	-0.350
σ'_f [MPa]	742	755
b	-0.066	-0.068
K' [MPa]	1251	1251
n'	0.194	0.194

2.2 Biaxial fatigue tests

Totally 10 biaxial fatigue tests were realized. In order to compare individual cases the amplitude of equivalent strain was calculated for each test as the minimal radius of the circumscribed circle in the diagram axial strain ε - equivalent value of shear strain ($\gamma/\sqrt{3}$). Similarly the amplitude of equivalent stress was calculated for each test as the minimal radius of the circumscribed circle in the diagram axial stress σ - efective shear stress ($\sqrt{3}\tau$). Main results of all biaxial tests are summarized in the Tab.3.

Tab. 3: Results of biaxial fatigue tests.

Spec. number	Path type	Axial strain amplit. ε_a [1]	Axial stress amplit. σ_a [MPa]	Eff. shear strain amplit. $\gamma_a/\sqrt{3}$ [1]	Eff. shear stress amplit. $\sqrt{3}\tau_a$ [MPa]	Equiv. strain amplit. ε_a^{eqv} [1]	Equiv. stress amplit. σ_a^{eqv} [MPa]	Number of cycles to failure N_f [1]
B11	torsion	0	0	0.0042	422	0.0042	422	6200
B1	torsion	0	0	0.0077	477	0.0077	477	1099
B10	torsion	0	0	0.0151	569	0.0151	569	416
B2	proport.	0.0055	348	0.0056	345	0.0078	490	818
B3	rhombic	0.0055	513	0.0056	554	0.0056	534	618
B4	circle	0.0075	689	0.0076	742	0.0075	715	434
B5	elliptic	0.0075	594	0.0076	649	0.0099	880	548
B7	2 blocks	0.0052	543	0.0052	551	0.0074	561	180
B8	square	0.0044	578	0.0047	617	0.0067	660	480
B6	square	0.0076	728	0.0076	780	0.0107	1067	108

2.2.1 Non-proportional hardening

Additional hardening of the material can be evaluated by the comparison of the amplitudes for proportional cases and non-proportional cases. Equivalent stress amplitudes for different loading paths are shown in the Fig.6.

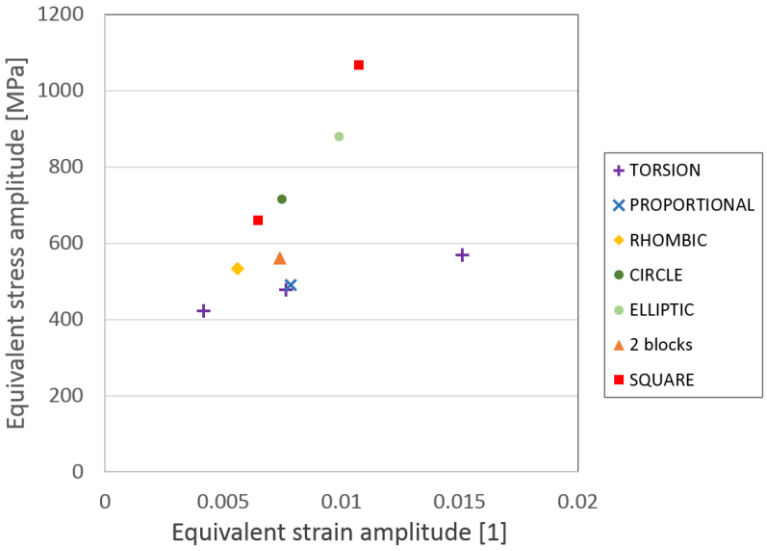

Fig. 6: Stress-strain diagram for different biaxial cases

The influence of strain path shape can be apparent from the Fig.7. All cases considered in the Fig.7 correspond to the same equivalent strain amplitude value of about 0.786 percent.

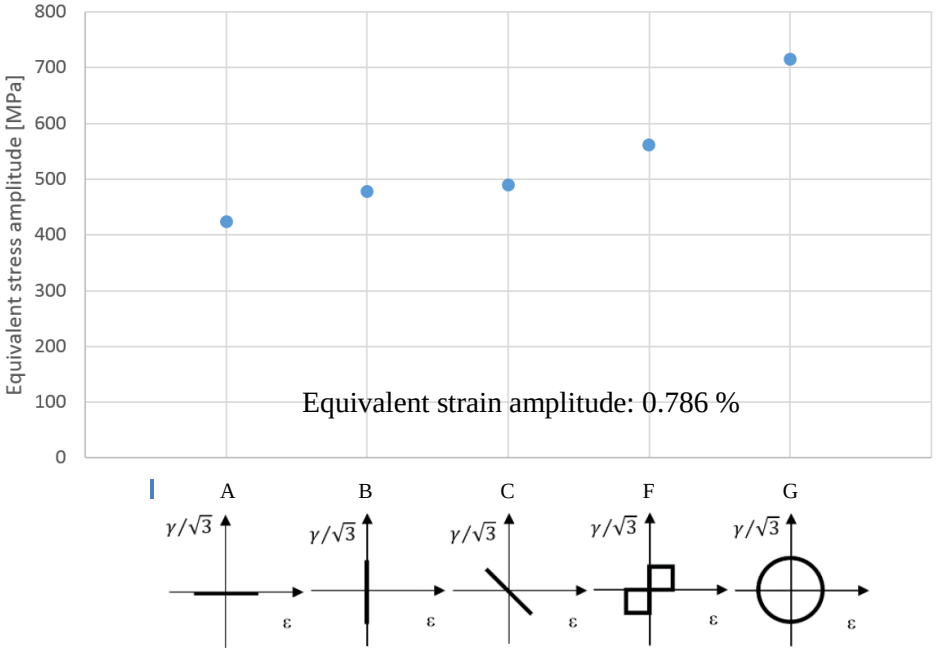

Fig. 7: Comparison of equivalent stress amplitude for different loading paths.

3 Discussion of results

The results of fatigue tests presented in the Fig.7 were obtained for a half life cycle. The smallest value of the equivalent stress amplitude is that of the uniaxial case. The slightly higher values were observed under torsion and proportional tension-torsion loading tests. Stronger additional hardening than in previous cases corresponds to the two block loading path, what is clear also from the Fig.6. The most significant additional hardening was observed under non-proportional 90° out-of-phase loading (about 69 per cent) and for square strain path shape, see Fig.6. The number of cycles to failure in the case of highly non-proportional loading is almost six times less than the number of cycles to failure under uniaxial loading with the same equivalent strain amplitude. A large amount of plastic work is accumulated, which ultimately leads to the lifetime shortening.

4 Conclusion

The main results from the fatigue tests realized on SS316L material under uniaxial as well as biaxial loading were presented. The cyclic hardening/softening curves shows similar behaviour on particular levels of strain amplitude. Very important conclusion of the experiments is, that really significant Non-Masing behaviour occurs. Regarding this fact a cyclic plasticity model with memory surface have to be used to describe the cyclic hardening/softening behaviour correctly. Each experimentally realized case has been simulated by the modified AbdelKarim-Ohno model [3] in the finite element program ANSYS 15.0. These results will be presented in a future paper.

Acknowledgement

This work was supported by The Ministry of Education, Youth and Sports from the National Programme of Sustainability (NPU II) project „IT4Innovations excellence in science - LQ1602", the project of specific research of Ministry of Education, Youth and Sports of the Czech Republic under No. SP2016/145 and by the Grant Agency of the Czech Republic (GACR), project No. 15-18274S.

References

[1] R. Halama, J. Sedlák, M. Šofer, Phenomenological Modelling of Cyclic Plasticity, in: P. Miidla (Ed.), Numerical Modelling, InTech, Rijeka, 2012, pp. 329-354.

[2] R. Halama, M. Šofer, F. Fojtík, Choice and Calibration of Cyclic Plasticity Model with Regard to Subsequent Fatigue Analysis. *Engineering Mechanics* 19 (2012) 87-97.

[3] R. Halama, F. Fojtík, A. Markopoulos, Memorization and Other Transient Effects of ST52 Steel and Its FE Description, *Applied Mechanics and Materials* 486 (2013) 48-53.

[4] Bäumel A. Seeger T. Material data for cyclic loading. supplement 1. materials science monographs. 61. Amsterdam: Elsevier Science. 1990.

[5] Ramberg W. Osgood WR. *Description of stress–strain curves by three parameters. Technical note no. 902*. Washington (DC): National Advisory Committee for Aeronautics. 1943.

[6] Niesłony A. El Dsoki Ch. Kaufmann H. Krug P. New method for evaluation of the Manson–Coffin–Basquin and Ramberg–Osgood equations with respect to compatibility. *International Journal of Fatigue* 30 (2008) 1967–77.